Acta Crystallographica Section F
Structural Biology and Crystallization Communications
ISSN 1744-3091

Crystallization and preliminary X-ray diffraction studies of a ferredoxin reductase from *Rhodopseudomonas palustris* CGA009

Ying Peng,[a] Feng Xu,[a]* Stephen G. Bell,[b] Luet-Lok Wong[b]* and Zihe Rao[a,c]

[a]Laboratory of Structural Biology, School of Medicine, Tsinghua University, Beijing 100084, People's Republic of China, [b]Department of Chemistry, University of Oxford, Inorganic Chemistry Laboratory, South Parks Road, Oxford OX1 3QR, England, and [c]National Laboratory of Biomacromolecules, Institute of Biophysics (IBP), Chinese Academy of Sciences, Beijing 100101, People's Republic of China

Correspondence e-mail: xuf@xtal.tsinghua.edu.cn, luet.wong@chem.ox.ac.uk

Received 5 March 2007
Accepted 9 April 2007

Palustrisredoxin reductase from *Rhodopseudomonas palustris* CGA009, a member of the oxygenase-coupled NADH-dependent ferredoxin reductase (ONFR) family, catalyzes electron transfer from NADH to ferredoxins. It is an essential component of the cytochrome P450 systems in *R. palustris* CGA009, a model organism with diverse metabolic pathways. Here, the crystallization of palustrisredoxin reductase is reported. The crystals belong to the trigonal space group $P3_221$, with unit-cell parameters a = 107.5, b = 107.5, c = 69.9 Å, and diffract to 2.2 Å resolution on a synchrotron source.

1. Introduction

Palustrisredoxin reductase (PuR) is an essential component of the soluble cytochrome P450 electron-transfer chains in *Rhodopseudomonas palustris* CGA009. PuR belongs to the oxygenase-coupled NADH-dependent ferredoxin reductase (ONFR) family of FAD-dependent electron-transfer enzymes [ferredoxin-NAD(P)H reductases; EC 1.18.1.3]. ONFRs not only support P450-dependent monooxygenation, but also the oxidation of hydrocarbons in the alkane hydroxylase and benzene/biphenyl dioxygenase systems (Senda *et al.*, 2000). Electron transport is initiated by a single two-electron transfer from NAD(P)H to FAD in ONFR to produce fully reduced $FADH_2$, which provides one electron to the iron–sulfur cluster, in most cases a [2Fe–2S] cluster, of ferredoxins. These electrons are finally transferred to the terminal oxygenase. Cytochrome P450 (CYP) enzymes are involved in the oxidative metabolism of both endogenous and exogenous compounds, including therapeutic drugs and other environmental toxins and carcinogens (Medina & Gómez-Moreno, 2004). These enzyme systems are of increasing interest for various applications, including the stereospecific synthesis of organic compounds and the degradation of pollutants (Sevrioukova *et al.*, 2004; Zanno *et al.*, 2005).

R. palustris is a purple photosynthetic bacterium that belongs to the α-proteobacteria and is widely distributed in nature. It has versatile metabolic pathways (Larimer *et al.*, 2004) and is capable of degrading numerous substituted aromatic acids and nitrogen-containing compounds, including amino acids and heterocyclic aromatic compounds. It also dehalogenates and degrades chlorinated benzoates and chlorinated fatty acids (McGrath & Harfoot, 1997; Egland *et al.*, 2001), which are found in industrial wastes. This organism has potential applications in waste recycling and biofuels because it can degrade and recycle diverse compounds including lignin monomers, fatty acids and dicarboxylic acids of the types derived from green plants, animal fats and seed oils. *R. palustris* contains seven CYP proteins: two ferredoxins (RPA1731 and RPA1872) that are associated with CYP genes and one putative ferredoxin reductase (RPA3782) that is not clustered with any CYP genes. The RPA3782 protein (palustrisredoxin reductase; PuR) has been expressed and found to associate with the RPA1872 ferredoxin to catalyze electron transfer to the RPA1871 (CYP199A2) cytochrome P450 enzyme. Full details of the cloning of the PuR gene and activity studies will be published separately.

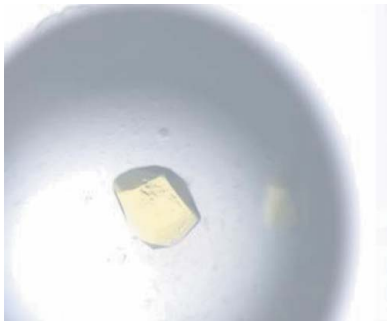

Two related crystal structures from the ONFR family have been solved to date: those of the ferredoxin-reductase component (BphA4) of biphenyl dioxygenase from *Pseudomonas* sp. strain KKS102 (Senda *et al.*, 2000) and putidaredoxin reductase from *P. putida* (Sevrioukova *et al.*, 2004). Unlike plant-type ferredoxin reductases, represented by spinach ferredoxin reductase, and thioredoxin reductases (TR), represented by adrenodoxin reductase (AdR), the topology of the two solved ONFR member structures is similar to the protein fold of the disulfide-reductase family (Sevrioukova *et al.*, 2004). The mechanism of electron transport of BphA4 has been studied and a model of the complex of putidaredoxin reductase and putidaredoxin has been proposed (Kuznetsov *et al.*, 2005). However, none of these studies has yielded the productive geometry of the flavin–nicotinamide interaction and the hydride-transfer mechanism in ONFR remains unclear. We hope that the structure of PuR will provide new information on these interactions. Here, we report the expression, purification, crystallization and dynamic light scattering of PuR. The results show that PuR forms a stable monomer and is suitable for crystallization.

2. Materials and methods

2.1. Expression and purification of wild-type PuR

PuR was overexpressed in the BL21(DE3) strain of *Escherichia coli* using the tandem *tac* promoters in the pCWori+ vector. Seed cultures of this strain harbouring the plasmid were grown overnight in 5 ml Luria–Bertani (LB) medium at 310 K with 100 µg ml^{-1} ampicillin. The 5 ml culture was inoculated into 1 l LB medium containing 100 µg ml^{-1} ampicillin and grown at 310 K. For functional expression, the cells were induced with 1 m*M* IPTG at an OD_{578} of ∼0.6 and cultivated for a further 3.5 h.

The cells were harvested by centrifugation. The pellets were bright yellow because of the FAD cofactor in the expressed protein. After resuspension in 40 ml buffer *A* (20 m*M* HEPES pH 7.0, 50 m*M* NaCl), cells were lysed by sonication on ice (medium power output). The debris was removed by centrifugation (30 min at 27 000*g*, 277 K) and the bright yellow supernatant was loaded onto a Fast Flow Q Sepharose column equilibrated with 20 m*M* HEPES pH 7.0. The protein was eluted with a linear gradient of NaCl in 20 m*M* HEPES pH 7.0 (Tris and other buffers were also tested, but it was found that HEPES pH 7.0 gave the best results). Yellow fractions were collected and desalted by passage through a G-25 column with 20 m*M* HEPES pH 7.0. The flowthrough was again loaded onto a Q-Sepharose column, washed and eluted with a 0.05–1 *M* NaCl gradient in 20 m*M* HEPES pH 7.0. The PuR protein fractions were collected, desalted on a G25 column and loaded onto a Resource Q (Amersham Biosciences) column pre-equilibrated with 20 m*M* HEPES pH 7.0 and eluted with a three-stage gradient (0.00–0.15, 0.15–0.45, 0.45–1 *M* NaCl) in 20 m*M* HEPES pH 7.0. PuR was eluted at ∼0.16 *M* NaCl. Fractions were collected, combined, concentrated and then loaded onto a Superdex 75 gel-filtration column pre-equilibrated and eluted with 20 m*M* HEPES pH 7.0, 150 m*M* NaCl. Fractions with $A_{280}/A_{458} < 6.5$ were collected and concentrated by ultrafiltration (30 kDa MWCO). Analysis by 12% SDS–PAGE showed the protein to have high purity and homogeneity (Fig. 1). The purified PuR (25 mg ml^{-1}) was stored in 20 m*M* HEPES pH 7.0. Protein concentration was estimated from direct absorbance at 280 nm using an extinction coefficient of $A_{280} = 0.552\ M^{-1}\ \mathrm{cm}^{-1}$.

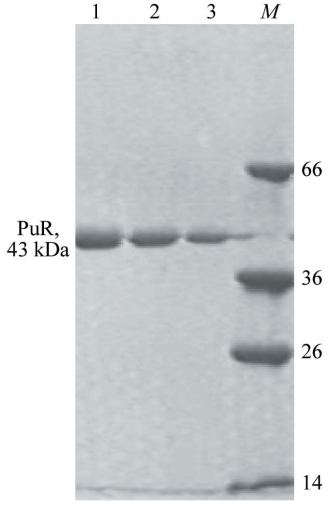

Figure 1
12% SDS–PAGE analysis of PuR purified using Superdex 75. Lanes 1–3 contain protein at different concentrations. Lane *M* contains molecular-weight markers (kDa).

2.2. Dynamic light scattering

Dynamic light scattering was performed using a DynaPro Titan dynamic light-scattering instrument (Wyatt Technology Corporation) that applied vertically polarized laser light of wavelength 829 nm. Light-scattering studies were carried out in the concentration range of 3–5 mg ml^{-1} PuR in 20 m*M* HEPES pH 7.0, 50 m*M* NaCl. Prior to DLS, all solvents were filtered through 0.2 µm membrane filters (Whatman) to remove dust particles; the solutions were centrifuged at 27 000*g* for 30 min and then filtered through 0.2 µm filters. The quartz cell was rinsed several times with filtered water and then filled with the filtered sample solution. The data obtained in each case were the average of ten runs, each of 10 s duration. The temperature was maintained at 289 K. Data were collected and analyzed using the *DYNAMICS* software for the DynaPro Titan instrument (Wyatt Technology Corporation). The DLS instrument was calibrated with BSA standard (2 mg ml^{-1} in PBS buffer, 298 K).

As shown in Fig. 2, the average size of PuR, as determined by DLS, was 3.1 nm, corresponding to a molecular weight of 49 kDa. Considering that the molecular weight calculated from sequence data is 43.7 kDa, we conclude that PuR is a monomer, which agrees with the results from gel-filtration experiments (data not shown). The observation of a monomodal distribution peak with a relatively

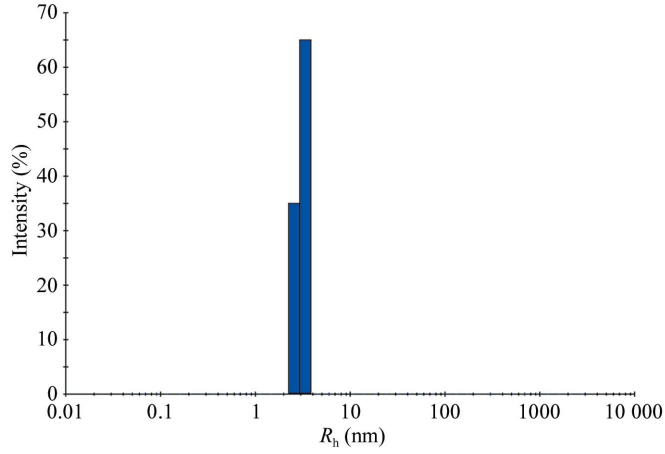

Figure 2
DLS measurements of PuR (5 mg ml^{-1}) in 20 m*M* HEPES pH 7.0, 50 m*M* NaCl. The average hydrodynamic radius was 3.1 nm.

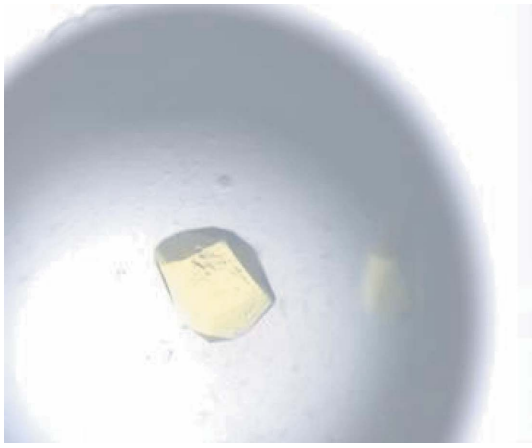

Figure 3
Crystal of PuR from *R. palustris* CGA009 grown by the hanging-drop vapour-diffusion method in 100 m*M* HEPES pH 7.2, 16%(*w*/*v*) polyethylene glycol (PEG) 10 000. Typical dimensions are approximately 0.3 × 0.3 × 0.2 mm.

narrow size distribution indicates that only one size of aggregation was found in the solution, which is identified as the monomer.

2.3. Crystallization of PuR

All crystallization procedures were carried out under aerobic conditions. The initial crystallization trials were carried out at 291 K in 16-well plates with Crystal Screen reagent kits I and II (Hampton Research) using the hanging-drop vapour-diffusion method. The droplets consisted of 1 µl 20 mg ml^{-1} protein in 20 m*M* HEPES pH 7.0 and 1 µl reservoir solution and were equilibrated against 200 µl reservoir solution. Initial spherulite crystals of PuR appeared in condition No. 38 [100 m*M* HEPES pH 7.5, 20%(*w*/*v*) PEG 10 000] of Crystal Screen II and this condition was used for further optimization by variation of precipitant concentration, buffer pH, protein concentration and temperature. PuR crystals suitable for X-ray diffraction were finally grown from 100 m*M* HEPES pH 7.0–7.2, 16–18%(*w*/*v*) PEG 10 000 at 291 K (Fig. 3). Crystals appeared after one week.

Table 1
Data-collection statistics.

Values in parentheses are for the outermost resolution shell.

Parameter	PuR
Wavelength (Å)	1.20
Space group	$P3_221$
Unit-cell parameters (Å, °)	a = 107.5, b = 107.5, c = 69.9, α = 90.000, β = 90.000, γ = 120.000
Resolution (Å)	50–2.20 (2.28–2.20)
Total observations	185683
Unique reflections	23724
Redundancy	7.8 (3.8)
Completeness (%)	98.8 (92.6)
$R_{\rm merge}$† (%)	7.0 (44.0)
Average $I/\sigma(I)$	19.51 (2.25)

† $R_{\rm merge} = \sum |I_i - \langle I \rangle| / \sum I$, where I_i is the intensity of the ith observation and $\langle I \rangle$ is the mean intensity of the reflections.

2.4. Data collection and processing

A single PuR crystal was harvested using a nylon loop (Hampton Research). Because of the high mosaicity of the crystals and the weak diffraction at high resolution, we transferred the crystal from the crystallization drop to 1 µl of a dehydration solution containing 20%(*w*/*v*) PEG 10 000, 100 m*M* HEPES pH 7.0 for 15 min. We also tried adding glycerol as a cryoprotectant; however, this did not prevent the appearance of ice rings. Using the Cryoscreen kit, we finally found 70 m*M* sodium cacodylate pH 6.5, 0.98 *M* sodium acetate, 30%(*v*/*v*) glycerol to be the best condition for cryoprotection. We transferred the crystal to the cryoprotection buffer for a few seconds. The crystal was then flash-cooled to 100 K in a nitrogen stream and used for data collection. A total of 186 images were collected using an oscillation of 1° per image on a MAR CCD detector on beamline 3W1A at the BSRF (Beijing Synchrotron

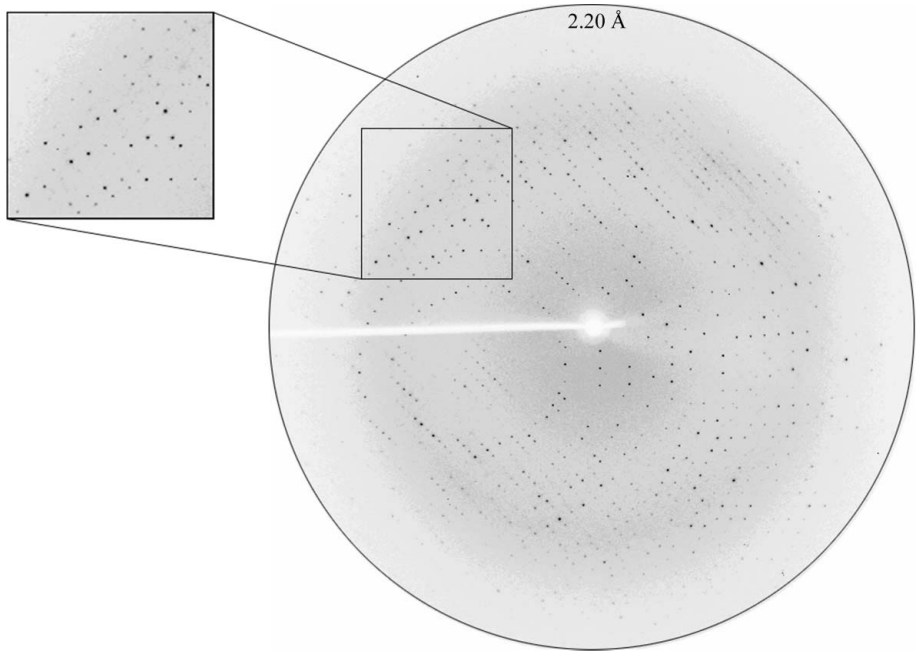

Figure 4
X-ray diffraction pattern of a PuR crystal, with a maximum resolution of 2.2 Å.

Radiation Facility) synchrotron-radiation source. Data were processed and scaled using the programs *DENZO* and *SCALEPACK* as implemented in the *HKL*-2000 package (Table 1).

3. Results and discussion

Initial attempts at obtaining diffraction from PuR crystals did not produce satisfactory data. Improvements were sought by varying the cryoprotection solution and dehydration conditions and a diffraction data set was finally collected to 2.2 Å resolution (Fig. 4). PuR crystals belonged to space group $P3_221$. Initial analysis of crystal solvent content using the Matthews coefficient (Matthews, 1968) suggested that the asymmetric unit contained one protein molecule with 53.5% solvent content (Matthews coefficient 2.7 $Å^3$ Da^{-1}). Molecular replacement using the structure of putidaredoxin reductase (PDB code 1q1w; 39% amino-acid sequence identity) as a search model was successfully carried out with *CNS* (Brünger *et al.*, 1998). Structural refinement is in progress.

This work was supported by grants from Project 863 of the Ministry of Science and Technology of China (grant No. 2005BA711A05-02) and the National Science Foundation of China (grant No. 30221003 to ZR) and grant EP-D048559-1 from the EPSRC and BBSRC, UK and the Higher Education Funding Council for England (to L-LW). We thank BSRF for supplying beamline time.

References

Brünger, A. T., Adams, P. D., Clore, G. M., DeLano, W. L., Gros, P., Grosse-Kunstleve, R. W., Jiang, J.-S., Kuszewski, J., Nilges, M., Pannu, N. S., Read, R. J., Rice, L. M., Simonson, T. & Warren, G. L. (1998). *Acta Cryst.* D**54**, 905–921.

Egland, P. G., Gibson, J. & Harwood, C. S. (2001). *Appl. Environ. Microbiol.* **67**, 1396–1399.

Kuznetsov, V. Y., Blair, E., Farmer, P. J., Poulos, T. L., Pifferitti, A. & Sevrioukova, I. F. (2005). *J. Biol. Chem.* **280**, 16135–16142.

Larimer, F. W., Chain, P., Hauser, L., Lamerdin, J., Malfatti, S., Do, L., Land, M. L., Pelletier, D. A., Beatty, J. T., Lang, A. S., Tabita, F. R., Gibson, J. L., Hanson, T. E., Bobst, C., Torres, J. L., Peres, C., Harrison, F. H., Gibson, J. & Harwood, C. S. (2004). *Nature Biotechnol.* **22**, 55–61.

McGrath, J. E. & Harfoot, C. G. (1997). *Appl. Environ. Microbiol.* **63**, 3333–3335.

Matthews, B. W. (1968). *J. Mol. Biol.* **33**, 491–497.

Medina, M. & Gómez-Moreno, C. (2004). *Photosyn. Res.* **79**, 113–131.

Senda, T., Yamada, T., Sakurai, N., Kubota, M., Nishizaki, T., Masai, E., Fukuda, M. & Mitsuidagger, Y. (2000). *J. Mol. Biol.* **304**, 397–410.

Sevrioukova, I. F., Li, H. & Poulos, T. L. (2004). *J. Mol. Biol.* **336**, 889–902.

Zanno, A., Kwiatkowski, N., Vaz, A. D. & Guardiola-Diaz, H. M. (2005). *Biochim. Biophys. Acta*, **1707**, 157–169.